Electronic Research Archive

http://www.aimspress.com/journal/era

ERA, 33(12): 7791–7809.
DOI: 10.3934/era.2025344
Received: 22 August 2025
Revised: 28 November 2025
Accepted: 02 December 2025
Published: 24 December 2025

Research article

Weighted modified Lindley model with WMLdist web application

Emrah Altun[1,*] **and Hana N. Alqifari**[2,*]

[1] Department of Statistics, Gazi University, Ankara 06560, Turkey

[2] Department of Statistics and Operations Research, College of Science, Qassim University, Buraydah 52571, Saudi Arabia

* **Correspondence:** Email: emrahaltun@gazi.edu.tr, hn.alqifari@qu.edu.sa.

Abstract: The gamma distribution is an essential distribution for modeling data in different areas such as insurance, finance, reliability, and many fields of engineering. This study proposes a new sophisticated distribution as an alternative to the gamma distribution with tractable properties. Mathematical characteristics and the parameter estimation process of the newly defined model are studied. Two datasets from two different disciplines, education and finance, are used to demonstrate the importance of the new model. Moreover, the WMLdist cloud-based application is developed to simplify and spread the use of the proposed distribution.

Keywords: gamma distribution; Lindley distribution; weighted distribution; simulation; software

1. Introduction

Right-skewed and positively defined random variables are modeled with gamma or Weibull distributions. Many generalizations of these distributions and competitive models have been studied by many authors. The Maxwell-Boltzmann-exponential (MBE) distribution of [1], the extended gamma distribution of [2], the generalized exponential distribution of [3], and the generalized gamma distribution of [4] can be viewed as alternative distributions to gamma and Weibull distributions. These distributions have a wide range of applications in finance, insurance, hydrology and life expectancy modeling. Wang et al. [5] studied the features of gusty wind with four probability distributions and found that the gamma model provided the best result. Chen et al. [6] investigated the optimal wind speed distribution for China and European regions and emphasized that the Weibull distribution is the best among the others; however, when the data have extreme values, the gamma and generalized extreme value distributions provide more accurate results than those of the Weibull distribution. Lencastre et al. [7] also examined other alternative distributions, especially the Weibull distribution, in modelling wind data, and interestingly, showed that the Gaussian distribution gives

better results. Mykhailenko et al. [8] carried out a very comprehensive study and calculated the wind energy potential with 10 different distributions. Their study [8] showed that the best distribution is the Weibull distribution.

Gamma and Weibull distributions have a wide range of applications in insurance. Marambakuyana and Shongwe [9] analyzed the risk of insurance claims under 19 different loss distributions. Hengcharoensuk and Moumeesri [10] calculated the ruin probability of an automobile insurance company using a new generalization of the gamma distribution. For other applications of the gamma distribution in insurance, the following studies can be examined: [11–14].

The gamma distribution is also used to analyze landslide and flood risks. Zhou and Zhang [15] analyzed flow duration curves using the gamma distribution for China. Montes-Pajuelo et al. [16] used the extreme value and gamma distributions to model extreme rainfall data. Shah and Pan [17] modeled the flood frequency distribution in India using the gamma distribution. Johar et al. [18] carried out an important study on modeling rainfall distribution using the gamma model.

Karuppusamy et al. [19] introduced a one-parameter modified Lindley (MoL) distribution and showed that the MoL distribution provides better results than the famous Lindley distribution. The fact that the MoL distribution gives better results than the Lindley distribution motivates us to introduce a weighted version of the MoL distribution. The Lindley distribution can be expressed as a mixture distribution of the exponential and gamma random variables with a fixed shape parameter value. Therefore, the flexibility of both the MoL and Lindley distributions is limited. To gain more flexibility in terms of bimodality and skewness, we use the weighted distribution approach to add one shape parameter to the baseline distribution, MoL. We call the proposed distribution the weighted MoL (WML) distribution. In this case, the resulting distribution has two parameters: One controls the shape of the distribution and the other one controls the range of the distribution.

The WML distribution is a more powerful distribution than the gamma distribution. The WML distribution has bimodal structures for the probability density function (PDF) and provides wider ranges for the dispersion measures than those of the gamma distribution. As in gamma distribution, the WML distribution has explicit mathematical expressions for its location and dispersion measures. Therefore, the WML distribution can be a good competitor of the gamma distribution in many applied fields such as hydrology, insurance, and renewable energy modeling.

In many applied fields, empirical data often display shapes that cannot be adequately captured by classical one-parameter or strictly unimodal lifetime distributions. Practical problems in reliability engineering, environmental sciences, biomedical studies, and risk modeling frequently involve datasets that exhibit heavier tails or bimodal behavior caused by heterogeneous subpopulations. The WML distribution is specifically designed to address these challenges. Its additional shape parameter allows the distribution to adapt to non-standard hazard patterns and multimodal structures while preserving analytical tractability. Such flexibility is especially valuable in reliability and survival.

The bimodal distribution is not a theoretical property but is a phenomenon that arises in real-life problems. For example, in mechanical systems, two distinct failure modes generate bimodal lifetime distributions. Similarly, in medical survival data, patients may belong to distinct risk groups, resulting in two characteristic survival peaks. Environmental variables such as daily wind speeds also commonly show dual or multi-regime behavior linked to seasonal or meteorological factors. Traditional unimodal models misrepresent such datasets and lead to biased parameter estimates and unreliable risk assessments. Therefore, the WML distribution provides an interpretable framework

that is capable of modeling complex, bimodal patterns that arise in real applications.

The rest of the paper is organized as follows: Section 2 deals with the properties of the WML distribution. In Section 3, the parameter estimation is analyzed with three different methods. In addition, these methods are compared for different sample sizes by a simulation study. In Section 4, the WML distribution is compared with popular distributions such as the gamma and Weibull distributions using two real data sets. In Section 5, the WMLdist program developed for the WML distribution is introduced. Section 6 concludes the study by emphasizing the important results of the model.

2. Modified weighted Lindley

We begin with the weighted Lindley (WL) distribution that was proposed by [20]. The PDF of the WL is

$$f(x;\alpha,b)=\frac{\alpha^{b+1}}{(\alpha+b)\,\Gamma(b)}x^{b-1}(1+x)\exp(-\alpha x), \tag{2.1}$$

where $\alpha, b, x > 0$, and $\Gamma(\cdot)$ is the gamma function. Ghitany et al. [20] used the following mathematical equation to introduce the WL distribution

$$f(x;\alpha,\mathbf{\Phi})=Dx^{\alpha-1}f(x;\mathbf{\Phi}), \tag{2.2}$$

where $f(x;\mathbf{\Phi})$ is the baseline distribution, $\mathbf{\Phi}$ is the parameter vector for the baseline model, and D is the constant term. In (2.2), the parameter α is the additional shape parameter that increases the flexibility of the baseline model. The baseline distribution is the Lindley distribution for the WL distribution.

Generating a weighted distribution in the form of (2.2) is useful when the baseline distribution has a simple form. The MoL distribution has only one scale parameter. Therefore, the development of a weighted form of the MoL distribution provides a flexible model with a high modeling capacity. Let X be a random variable following the MoL distribution with the following PDF:

$$f(x;\theta)=\frac{\theta^4}{\theta^3+6}\left(1+x^3\right)\exp(-\theta x), \tag{2.3}$$

where $\theta > 0$ is the scale parameter. We have the following proposition for the construction of the WML distribution.

Proposition 1. *The WML is defined by*

$$f(x;\alpha,\theta)=\frac{\left(x^3+1\right)\theta^{\alpha+3}x^{\alpha-1}\exp(-\theta x)}{\Gamma(\alpha)\left(\alpha^3+3\alpha^2+2\alpha+\theta^3\right)}, \tag{2.4}$$

where $\alpha > 0$ is an additional shape parameter and $\Gamma(\cdot)$ is the gamma function.

Proof. The constant term, D, is obtained by

$$
\begin{aligned}
D^{-1} &= \int_0^\infty x^{\alpha-1}\frac{\theta^4}{\theta^3+6}\left(1+x^3\right)\exp\left(-\theta x\right)dx,\\
&= \int_0^\infty \frac{\theta^4 x^{\alpha-1}\exp\left(-\theta x\right)}{\theta^3+6}dx+\int_0^\infty \frac{\theta^4 x^{\alpha+2}\exp\left(-\theta x\right)}{\theta^3+6}dx,\\
&= \frac{\theta^4\Gamma\left(\alpha\right)}{\left(\theta^3+6\right)\theta^\alpha}+\frac{\theta^4\Gamma\left(\alpha+3\right)}{\left(\theta^3+6\right)\theta^{\alpha+3}},\\
&= \frac{\theta^7\Gamma\left(\alpha\right)+\theta^4\Gamma\left(\alpha+3\right)}{\left(\theta^3+6\right)\theta^{\alpha+3}},\\
&= \frac{\theta^4\left(\theta^3\Gamma\left(\alpha\right)+\Gamma\left(\alpha+3\right)\right)}{\left(\theta^3+6\right)\theta^{\alpha+3}},\\
&= \frac{\theta^4\left(\alpha^3+3\alpha^2+2\alpha+\theta^3\right)\Gamma\left(\alpha\right)}{\left(\theta^3+6\right)\theta^{\alpha+3}}.
\end{aligned}
\tag{2.5}
$$

Therefore, the normalizing constant is

$$
D=\frac{\left(\theta^3+6\right)\theta^{\alpha+3}}{\theta^4\left(\alpha^3+3\alpha^2+2\alpha+\theta^3\right)\Gamma\left(\alpha\right)}. \tag{2.6}
$$

Using (2.2) and (2.6), we have

$$
f\left(x;\alpha,\theta\right)=\frac{\left(x^3+1\right)\theta^{\alpha+3}x^{\alpha-1}\exp\left(-\theta x\right)}{\Gamma\left(\alpha\right)\left(\alpha^3+3\alpha^2+2\alpha+\theta^3\right)}. \tag{2.7}
$$

The WML distribution has bimodal and right-skewed shapes. The WML distribution reduces to MoL distribution for $\alpha = 1$.

Proposition 2. *The cumulative distribution function (CDF) of 2.4 is*

$$
F\left(x\right)=\frac{\theta^{\alpha+3}}{\left(\alpha^3+3\alpha^2+2\alpha+\theta^3\right)\Gamma\left(\alpha\right)}\left(\frac{\gamma\left(\alpha,\theta x\right)}{\theta^\alpha}+\frac{\gamma\left(\alpha+3,\theta x\right)}{\theta^{\alpha+3}}\right), \tag{2.8}
$$

where $\gamma\left(\cdot,\cdot\right)$ is the lower incomplete gamma function.

Proof. Let $A=\frac{\theta^{\alpha+3}}{\left(\alpha^3+3\alpha^2+2\alpha+\theta^3\right)\Gamma\left(\alpha\right)}$, we have

$$
\begin{aligned}
F(x) &= A\int_0^x\left(1+t^3\right)t^{\alpha-1}\exp\left(-\theta t\right)dt,\\
&= A\left(\underbrace{\int_0^x t^{\alpha-1}\exp\left(-\theta t\right)dt}_{I}+\underbrace{\int_0^x t^{\alpha+2}\exp\left(-\theta t\right)dt}_{II}\right).
\end{aligned}
\tag{2.9}
$$

Consider the first integral integral

$$I(x) = \int_0^x t^{\alpha-1} e^{-\theta t}\, dt. \tag{2.10}$$

Let $u = \theta t$ and $du = \theta dt$. When $t = 0$, $u = 0$ and when $t = x$, $u = \theta x$. Using these changes in the variables, the integral is

$$\begin{aligned} I(x) &= \int_0^{\theta x} \left(\frac{u}{\theta}\right)^{\alpha-1} e^{-u}\, \frac{du}{\theta}, \\ &= \theta^{-(\alpha-1)}\theta^{-1} \int_0^{\theta x} u^{\alpha-1} e^{-u}\, du, \\ &= \theta^{-\alpha} \int_0^{\theta x} u^{\alpha-1} e^{-u}\, du. \end{aligned} \tag{2.11}$$

The lower incomplete gamma function is defined as

$$\gamma(\alpha, z) = \int_0^z u^{\alpha-1} e^{-u}\, du.$$

Therefore, the integral in (2.11) is

$$\int_0^x t^{\alpha-1} e^{-\theta t}\, dt = \theta^{-\alpha}\, \gamma(\alpha, \theta x).$$

Consider the second integral

$$I(x) = \int_0^x t^{\alpha+2} e^{-\theta t}\, dt. \tag{2.12}$$

Using the same change in variables, we have

$$\begin{aligned} I(x) &= \int_0^{\theta x} \left(\frac{u}{\theta}\right)^{\alpha+2} e^{-u}\, \frac{du}{\theta}, \\ &= \theta^{-(\alpha+2)}\theta^{-1} \int_0^{\theta x} u^{\alpha+2} e^{-u}\, du, \\ &= \theta^{-(\alpha+3)} \int_0^{\theta x} u^{\alpha+2} e^{-u}\, du. \end{aligned} \tag{2.13}$$

Recall the lower incomplete gamma function

$$\gamma(s, z) = \int_0^z u^{s-1} e^{-u}\, du.$$

Putting $s = \alpha + 3$, we have $\displaystyle\int_0^{\theta x} u^{\alpha+2} e^{-u}\, du = \gamma(\alpha + 3, \theta x)$. Therefore, the second part of the integral is

$$\int_0^x t^{\alpha+2} e^{-\theta t}\, dt = \theta^{-(\alpha+3)}\, \gamma(\alpha + 3, \theta x).$$

Inserting both integral results and putting A into (2.9), we have

$$F(x) = \frac{\theta^{\alpha+3}}{(\alpha^3 + 3\alpha^2 + 2\alpha + \theta^3)\Gamma(\alpha)} \left(\frac{\gamma(\alpha, \theta x)}{\theta^{\alpha}} + \frac{\gamma(\alpha + 3, \theta x)}{\theta^{\alpha+3}} \right). \tag{2.14}$$

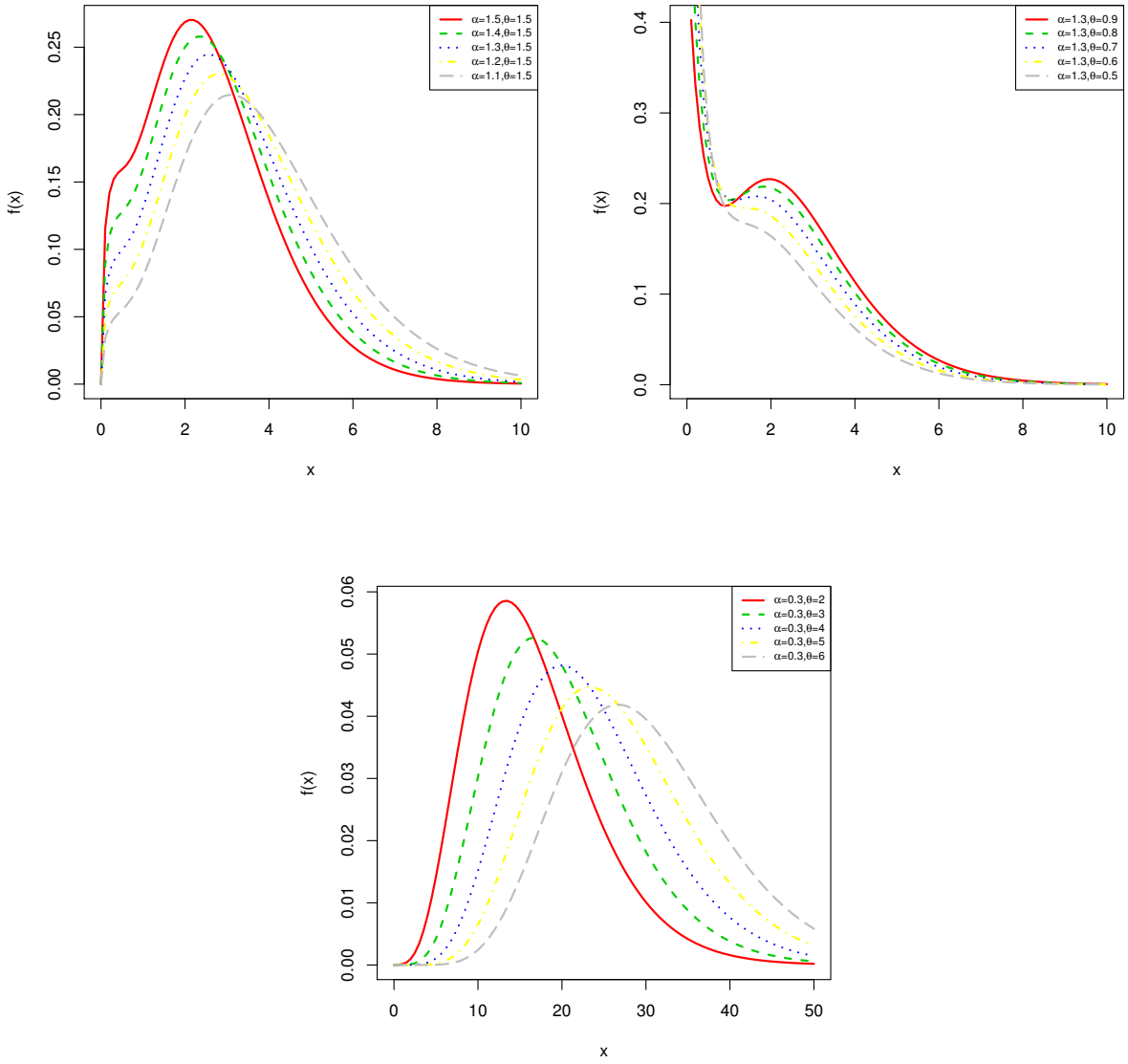

Figure 1. PDF shapes.

The flexibility of the WML model in terms of PDF is shown in Figure 1. The WML distribution, with the flexibility provided by the extra shape parameter, yields quite successful results in modelling data with different characteristic properties.

2.1. Moments

The moments and related measures of the WML model are discussed. We have the following result for the raw moments of the WML model.

Proposition 3. *The rth raw moment of X is*

$$E\left(X^r\right) = \frac{\Gamma\left(\alpha + r\right)\theta^3 + \Gamma\left(\alpha + (r+3)\right)}{\theta^r \Gamma\left(\alpha\right)\left(\alpha^3 + 3\alpha^2 + 2\alpha + \theta^3\right)}. \tag{2.15}$$

Proof. The rth raw moment of X is

$$\begin{aligned} E\left(X^r\right) &= A\int_0^\infty x^r\left(1 + x^3\right)x^{\alpha-1}\exp\left(-\theta x\right)dx \\ &= A\left(\int_0^\infty x^{r+\alpha-1}\exp\left(-\theta x\right)dx + \int_0^\infty x^{r+\alpha+2}\exp\left(-\theta x\right)dx\right). \end{aligned} \tag{2.16}$$

Let $u = \theta x$ and apply both integrals, we can obtain

$$\int_0^\infty x^{r+\alpha-1}e^{-\theta x}\,dx = \theta^{-(r+\alpha)}\Gamma(r+\alpha), \tag{2.17}$$

$$\int_0^\infty x^{r+\alpha+2}e^{-\theta x}\,dx = \theta^{-(r+\alpha+3)}\Gamma(r+\alpha+3). \tag{2.18}$$

Combining both results, we have

$$\int_0^\infty \left(x^{r+\alpha-1}e^{-\theta x} + x^{r+\alpha+2}e^{-\theta x}\right)dx = \theta^{-(r+\alpha)}\Gamma(r+\alpha) + \theta^{-(r+\alpha+3)}\Gamma(r+\alpha+3). \tag{2.19}$$

Inserting these results into (2.16), we have

$$E\left(X^r\right) = \frac{\theta^3\Gamma\left(r+\alpha\right) + \Gamma\left(r+\alpha+3\right)}{\left(\alpha^3 + 3\alpha^2 + 2\alpha + \theta^3\right)\Gamma\left(\alpha\right)\theta^r}. \tag{2.20}$$

Putting $r = 1$ and $r = 2$ in (2.15), we have

$$E\left(X\right) = \frac{\theta^3\Gamma\left(1+\alpha\right) + \Gamma\left(\alpha+4\right)}{\left(\alpha^3 + 3\alpha^2 + 2\alpha + \theta^3\right)\Gamma\left(\alpha\right)\theta}, \tag{2.21}$$

$$E\left(X^2\right) = \frac{\theta^3\Gamma\left(2+\alpha\right) + \Gamma\left(\alpha+5\right)}{\left(\alpha^3 + 3\alpha^2 + 2\alpha + \theta^3\right)\Gamma\left(\alpha\right)\theta^2}. \tag{2.22}$$

The variance of X is

$$\mathrm{Var}\left(X\right) = \frac{\Gamma\left(\alpha+2\right)\,\theta^3 + \Gamma\left(\alpha+5\right)}{\theta^2\,\Gamma\left(\alpha\right)\,\left(\alpha^3 + 3\,\alpha^2 + 2\,\alpha + \theta^3\right)} - \frac{\left(\Gamma\left(\alpha+1\right)\,\theta^3 + \Gamma\left(\alpha+4\right)\right)^2}{\theta^2\,\Gamma\left(\alpha\right)^2\left(\alpha^3 + 3\,\alpha^2 + 2\,\alpha + \theta^3\right)^2}. \tag{2.23}$$

Due to the complexity of the skewness and kurtosis equations in the WML model, these equations are not presented here. Nevertheless, Figure 2 illustrates how the skewness and kurtosis values vary with different parameter values. Furthermore, Figure 2 also analyzes the changes in the mean and variance values in relation to the parameters. We have the following results.

✓ As the parameter α increases, the mean and variance increase, while the skewness and kurtosis decrease.

✓ As the parameter θ increases, the mean and variance decrease, while the skewness and kurtosis increase.

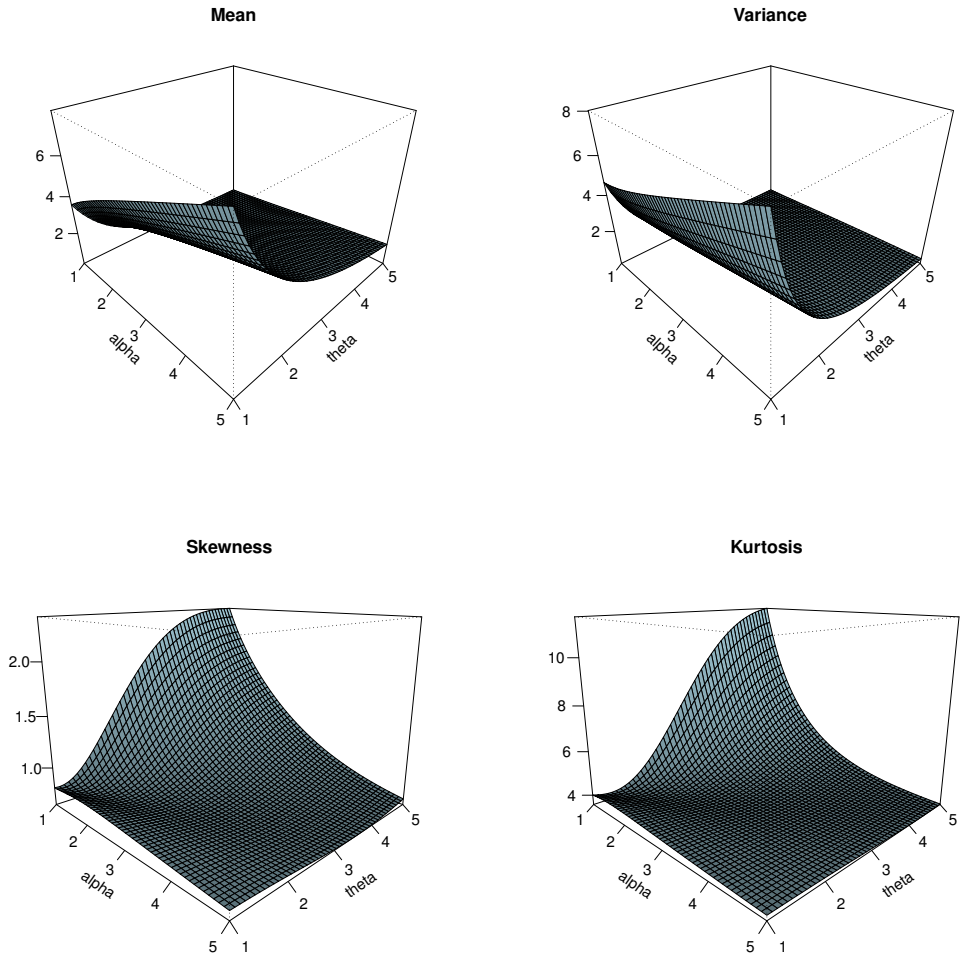

Figure 2. Plots for moments and related measures.

2.2. Lorenz curve

The Lorenz curve (LC) is defined by

$$L(x) = \frac{\int_0^x t f(t)\, dt}{\mu}, \tag{2.24}$$

where μ and $f(\cdot)$ are defined in (2.21) and (2.4). To calculate the LC for the WML, we use the expanded form of the PDF, as follows:

$$f(x;\alpha,\theta)=\frac{\theta^{\alpha+3}x^{\alpha-1}\exp(-\theta x)}{\Gamma(\alpha)\left(\theta^3+\alpha(\alpha+1)(\alpha+2)\right)}+\frac{\theta^{\alpha+3}x^{\alpha+2}\exp(-\theta x)}{\Gamma(\alpha)\left(\theta^3+\alpha(\alpha+1)(\alpha+2)\right)}. \tag{2.25}$$

Using (2.25), we have

$$\int_0^x tf(t)\,dt=A\left(\int_0^x t^{\alpha}\exp(-\theta t)dt+\int_0^x t^{\alpha+3}\exp(-\theta t)dt\right). \tag{2.26}$$

Using the same change in the variables in Proposition 2 and the properties of the lower incomplete gamma function, one can obtain

$$\int_0^x t^{\alpha}\exp(-\theta t)dt = \frac{\gamma(\alpha+1,\theta x)}{\theta^{\alpha+1}}, \tag{2.27}$$

$$\int_0^x t^{\alpha+3}\exp(-\theta t)dt = \frac{\gamma(\alpha+4,\theta x)}{\theta^{\alpha+4}}. \tag{2.28}$$

Inserting these results into (2.26), we have

$$\int_0^x tf(t)\,dt=\frac{\theta^{\alpha+3}}{\left(\alpha^3+3\alpha^2+2\alpha+\theta^3\right)\Gamma(\alpha)}\left(\frac{\gamma(\alpha+1,\theta x)}{\theta^{\alpha+1}}+\frac{\gamma(\alpha+4,\theta x)}{\theta^{\alpha+4}}\right). \tag{2.29}$$

Note that (2.29) is the first incomplete moments of the WML distribution. So, the LC is

$$L(x)=\frac{\theta^{\alpha+4}}{\theta^3\Gamma(1+\alpha)+\Gamma(\alpha+4)}\left(\frac{\gamma(\alpha+1,\theta x)}{\theta^{\alpha+1}}+\frac{\gamma(\alpha+4,\theta x)}{\theta^{\alpha+4}}\right). \tag{2.30}$$

2.3. Hazard shapes

The hazard shapes of the WML distribution is investigated graphically. The hazard rate function (HRF) of the WML is

$$h(x)=\frac{\theta^{\alpha+3}\left(1+x^3\right)x^{\alpha-1}\exp(-\theta x)}{\left(\alpha^3+3\alpha^2+2\alpha+\theta^3\right)\Gamma(\alpha)-\theta^3\gamma(\alpha,\theta x)-\gamma(\alpha+3,\theta x)}. \tag{2.31}$$

Figure 3 shows the hazard regions of the WML distribution for different parameter values. The results show that the WML distribution has two different hazard structures. These are the increasing and bathtub shapes.

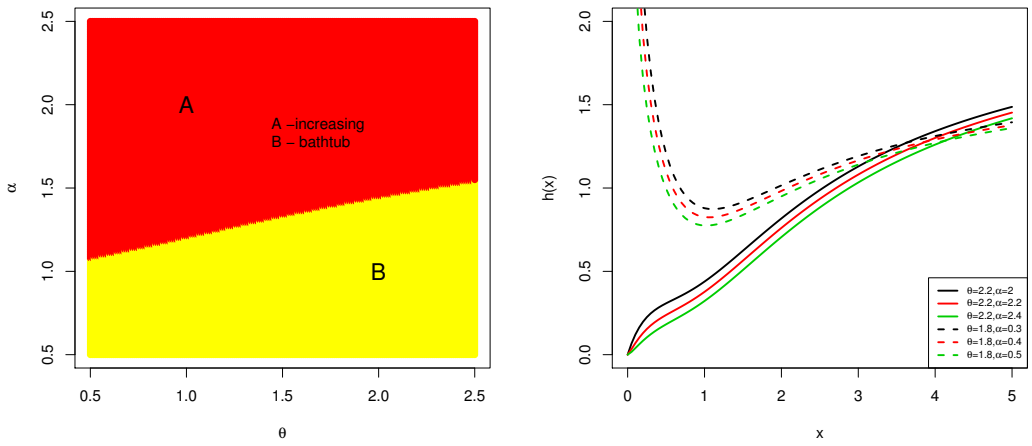

Figure 3. HRF shapes.

2.4. Data generation

We employ the inverse transform method to produce random variables derived from the WML distribution. This technique relies on solving the equation $F(x) = u$, where $u \sim \mathrm{U}(0,1)$. In general, an explicit solution for $F(x) = u$ is not available. In such instances, a nonlinear equation solver is utilized. In this context, we utilize the solve function in R to address the nonlinear equation $F(x) = u$. The algorithm outlined below can be implemented to generate n random observations from the WML distribution.

1) Determine the values of the α and θ.

2) Generate u from $U(0,1)$.

3) Solve the equation using the **solve** function in R.

$$\frac{\theta^{\alpha+3}}{(\alpha^3+3\alpha^2+2\alpha+\theta^3)\,\Gamma(\alpha)}\left(\frac{\gamma(\alpha,\theta x)}{\theta^{\alpha}}+\frac{\gamma(\alpha+3,\theta x)}{\theta^{\alpha+3}}\right)-u=0$$

4) Repeat Steps 2 and 3 n times.

3. Estimation and simulation

Three estimation methods are used. These are the maximum likelihood (ML), least squares (LS), and weighted LS (WLS) methods. First, we begin with the ML estimation (MLE) method. The log-likelihood function of the WML model is

$$\begin{aligned}\ell(\alpha,\theta) &= \sum_{i=1}^{n}\log\left(x_i^3+1\right)+n(\alpha+3)\log(\theta)+(\alpha-1)\sum_{i=1}^{n}\log(x_i)-\theta n\bar{x}\\ &- n\log\Gamma(\alpha)-n\log\left(\alpha^3+3\alpha^2+2\alpha+\theta^3\right).\end{aligned}\tag{3.1}$$

Partial derivatives of (3.1) are

$$I_\alpha = n\log\theta + \sum_{i=1}^{n}\log(x_i) + n\psi(\alpha) - n\left(\frac{3\alpha^2+6\alpha+2}{\alpha^3+3\alpha^2+2\alpha+\theta^3}\right), \tag{3.2}$$

$$I_\theta = \frac{3n(\alpha+3)}{\theta} - n\bar{x} - n\left(\frac{3\theta^2}{\alpha^3+3\alpha^2+2\alpha+\theta^3}\right), \tag{3.3}$$

where $\psi(\alpha)$ is the digamma function. If the partial derivatives given in Eqs (3.2) and (3.3) are set equal to 0 and solved simultaneously, MLEs are obtained. However, closed-form MLEs cannot be obtained from the solution of these equations together. Therefore, it is necessary to maximize the function given in Eq (3.1) to obtain MLEs.

The asymptotic standard errors of the estimated parameters of the WML model is obtained using the observed information matrix (OIM). The elements of the OIM are given by

$$I_{\alpha\alpha} = n\frac{\left(3\alpha^2+6\alpha+2\right)\left(3\alpha^2+6\alpha+2\right) - (6\alpha+6)\left(\alpha^3+3\alpha^2+2\alpha+\theta^3\right)}{\left(\alpha^3+3\alpha^2+2\alpha+\theta^3\right)^2} + n\psi^{(1)}(\alpha), \tag{3.4}$$

$$I_{\theta\theta} = n\left(\frac{\left(3\alpha^2+6\alpha+2\right)3\theta^2 - 6\theta\left(\alpha^3+3\alpha^2+2\alpha+\theta^3\right)}{\left(\alpha^3+3\alpha^2+2\alpha+\theta^3\right)^2}\right) - \frac{3n}{\theta^2}, \tag{3.5}$$

$$I_{\theta\alpha} = I_{\alpha\theta} = \frac{n\left(3\alpha^2+6\alpha+2\right)3\theta^2}{\left(\alpha^3+3\alpha^2+2\alpha+\theta^3\right)^2}, \tag{3.6}$$

where $\psi^{(1)}(\alpha)$ is the first derivative of the digamma function. Besides the MLE method, the effectiveness of the LS and WLS methods in deriving the parameter estimates of the WML distribution is also investigated. The LS and WLS estimators of the parameters of the WML distribution are obtained by minimizing the functions given in Eqs (3.7) and (3.8).

$$\sum_{i=1}^{j}\left[F\left(x_{i:j};\alpha,\theta\right) - \frac{i}{j+1}\right]^2, \tag{3.7}$$

$$\sum_{i=1}^{j}\frac{(j+1)^2(j+2)}{i(j-i+1)}\left[F\left(x_{i:j};\alpha,\theta\right) - \frac{i}{j+1}\right]^2, \tag{3.8}$$

where $F\left(x_{i:j};\alpha,\theta\right)$ is in (2.8) and $x_{i:j}$ is the ith-order statistic.

3.1. Simulation

In the simulation section, the success of the MLE, LSE, and WLSE methods in the parameter estimation process is compared. The number of simulation repetitions is set at 1000. Three cases are investigated. These are as follows:

- ✓ Case I: $\alpha = 0.5, \theta = 0.5$,
- ✓ Case II: $\alpha = 0.5, \theta = 2$,

✓ Case III: $\alpha = 3, \theta = 3$.

The results are given in Table 1. The simulation results are interpreted according to the bias and mean squared error (MSE) values obtained as a result of 1000 repetitions. We have the following results. For the first case, the MLE consistently exhibits the smallest MSE values for both parameters across all sample sizes. Although the LSE and WLSE achieve slightly smaller bias in some cases, their MSE values remain noticeably higher, especially for small and moderate samples. As expected, all estimators show an improvement as the sample size increases, indicating convergence towards the true parameter values. The WLSE performs better than the LSE in terms of MSE but remains inferior to the MLE. Under the second case, a similar pattern persists. The MLE continues to dominate in terms of MSE for both α and θ, while the LSE displays slightly lower bias for α at certain sample sizes but at the cost of increased variability. In the third case, all estimators show increased bias and MSE for $n = 100$, but performance stabilizes as the sample size grows. The MLE continues to yield the smallest MSE for θ and is competitive for α particularly for $n = 300$ and $n = 500$. Although the WLSE provides bias improvements in some instances, its overall MSE remains higher than that of the MLE. Overall, the simulation results demonstrate that the MLE is the most efficient estimator for the WML distribution, especially in terms of MSE, while the LSE and WLSE may offer marginal bias reductions at the expense of greater variability. These findings support the use of the MLE as the primary estimation method in practical applications of the WML distribution.

Table 1. Simulation results.

Cases	Sample sizes	Metrics	MLE		LSE		WLSE	
			α	θ	α	θ	α	θ
I	100	Bias	0.06134	0.01086	0.03711	0.00382	0.04273	0.00608
		MSE	0.03405	0.00177	0.06789	0.00299	0.05024	0.00229
	300	Bias	0.01416	0.00327	0.00641	0.00128	0.00874	0.00201
		MSE	0.00695	0.00044	0.01718	0.00088	0.01100	0.00061
	500	Bias	0.01130	0.00184	0.02034	0.00319	0.01622	0.00264
		MSE	0.00367	0.00024	0.01242	0.00054	0.00745	0.00036
II	100	Bias	0.01652	0.05196	0.00138	0.01311	0.00465	0.02265
		MSE	0.00327	0.03475	0.00412	0.04091	0.00346	0.03469
	300	Bias	0.01025	0.02857	-0.00065	0.00294	0.00308	0.01414
		MSE	0.00111	0.01115	0.00144	0.01389	0.00112	0.01134
	500	Bias	0.00959	0.02167	-0.00162	-0.00397	0.00313	0.00993
		MSE	0.00064	0.00640	0.00076	0.00822	0.00059	0.00659
III	100	Bias	0.10461	0.07909	0.02692	0.02056	0.05411	0.04142
		MSE	0.20806	0.10539	0.32000	0.15022	0.24564	0.11959
	300	Bias	0.01359	0.00508	-0.01288	-0.01176	-0.00061	-0.00373
		MSE	0.05717	0.02776	0.08496	0.04207	0.06561	0.03250
	500	Bias	0.02412	0.01538	0.00955	0.00465	0.01628	0.00968
		MSE	0.04037	0.01920	0.06157	0.02902	0.04803	0.02275

4. Applications

Two real datasets are analyzed. The WML distribution is compared with the gamma, Weibull, and WL distributions. Goodness-of-fit tests, Kolmogorov Smirnov (KS), Anderson Darling (AD), and Cramer von-Mises (CVM), are implemented on the selected data sets. Moreover, two famous information criteria, the Akaike information criterion (AIC) and the Bayesian information criterion (BIC), are used to determine the best-fitted model.

4.1. Study time

The data used in the first application is related to the study time of 100 students. The dataset is available at www.kaggle.com/datasets/yasserh/student-marks-dataset/data. The data are modeled with WML, gamma, Weibull, and WL distributions and the results are given in Table 2. According to the results obtained, the WML distribution gives more successful results than the other competitive models in modeling the data. The model comparison metrics, such as AIC, BIC, AD, CVM, and KS, obtained for the WML distribution are lower than those of other models. Therefore, the WML distribution is chosen as the best model.

Table 2. Results for the study time data.

Models	Parameter estimations		$-\ell$	AIC	BIC	AD	CVM	KS	p-value
WML (α, θ)	0.765	0.827	223.978	451.956	457.166	1.294	0.173	0.106	0.213
	0.149	0.063							
Gamma (α, θ)	1.701	0.417	233.271	470.542	475.753	2.912	0.453	0.145	0.030
	0.221	0.063							
Weibull (α, θ)	1.589	4.486							
	0.136	0.294	228.345	460.689	460.813	2.060	0.303	0.110	0.179
WL (α, b)	0.491	1.281							
	0.063	0.207	230.616	465.232	470.442	2.446	0.371	0.133	0.057

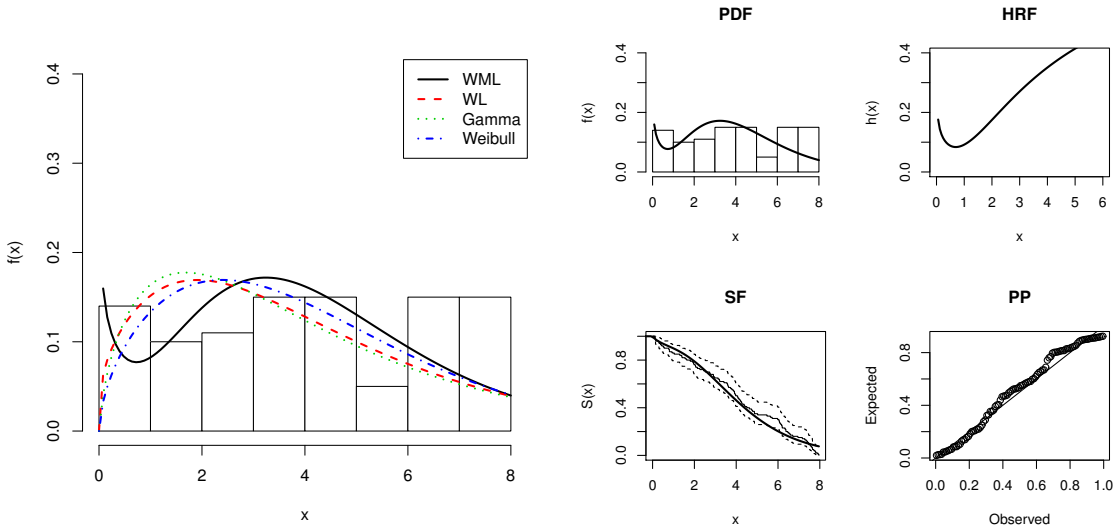

Figure 4. Fitted densities for the study time data.

In Figure 4, the estimated PDFs for all distributions are shown on the histogram data. On the right side of Figure 4, the PDF, survival, and hazard functions, and probability-probability (PP) graphs obtained for the WML distribution are given. These graphs show the adequate fit of the WML distribution to the data.

4.2. Poverty rate

The dataset used for the second application is about the poverty rates of 14 Southern African and Middle Eastern countries. The data can be accessed at www.kaggle.com/datasets/towhid121/sa-me-happiness-index. This data are modeled with the same distributions as in the first application, and the results are given in Table 3. Since the WML distribution has the lowest values of the model selection criteria, it is selected as the best model for the second dataset. In addition, the results given in Figure 5 clearly demonstrate the excellent fit of the WML distribution to the data.

Table 3. Results for the poverty rate data.

Models	Parameter estimations		$-\ell$	AIC	BIC	AD	CVM	KS	p-value
WML (α, θ)	0.081	0.157	52.879	109.757	111.035	0.426	0.069	0.153	0.850
	0.106	0.025							
Gamma (α, θ)	1.283	0.067	55.118	114.236	115.514	1.110	0.192	0.286	0.166
	0.436	0.028							
Weibull (α, θ)	1.341	20.498	54.589	113.178	114.456	0.974	0.168	0.246	0.310
	0.292	4.225							
WL (α, b)	0.080	0.641	53.886	111.772	113.050	0.821	0.141	0.265	0.235
	0.027	0.370							

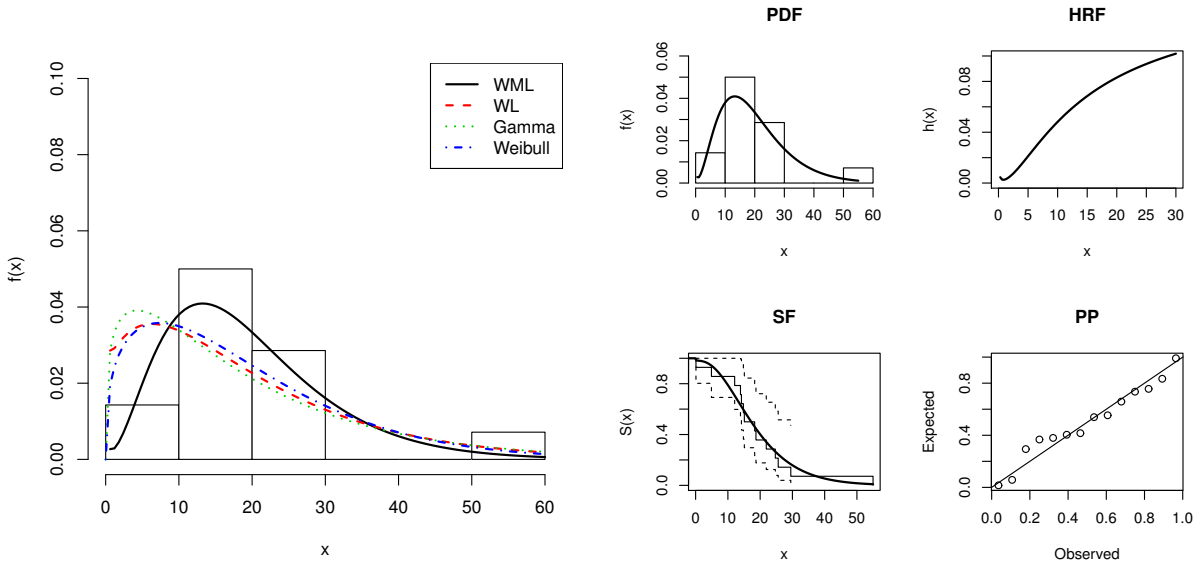

Figure 5. Fitted densities for the poverty rate data.

5. Software

R Shiny is a powerful tool to make complex statistical models easy for the users. Many researchers use the R Shiny program to develop user-friendly cloud-based applications such as LTPL by [21], DataVis2 by [22], and SimBetaReg by [23].

In this section, the WMLdist web-tool is introduced. WMLdist is a cloud-based application specially developed in R Shiny for WML distribution. Thanks to WMLdist, the application of the WML distribution on a real data set can be done easily. The WMLdist is accessible at https://gazistat.shinyapps.io/WMLdist/.

Figure 6 shows the data upload section of WMLdist. Here, the user can upload his/her own data or choose one of the two available datasets. The datasets given here are the datasets used in the application section of the study.

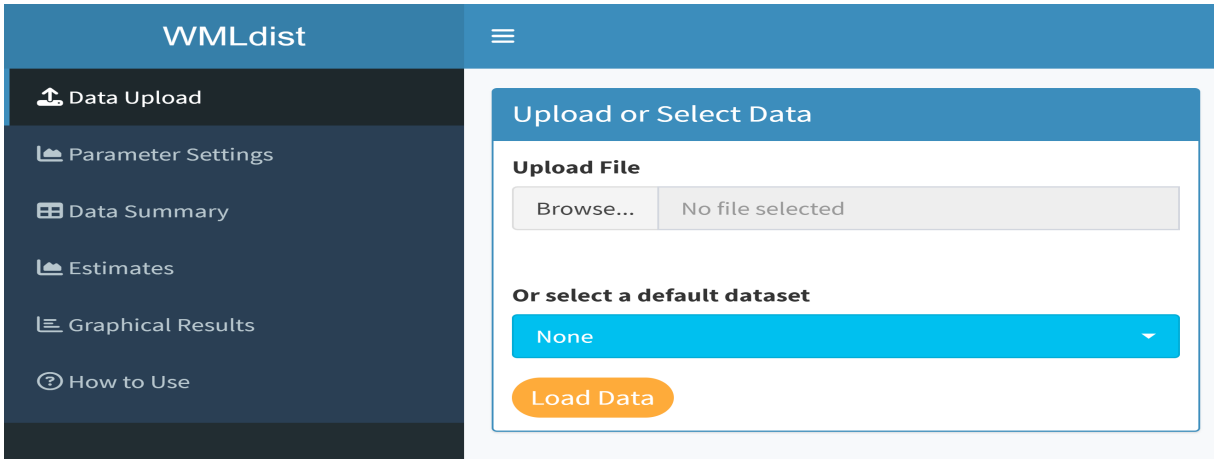

Figure 6. Upload data panel.

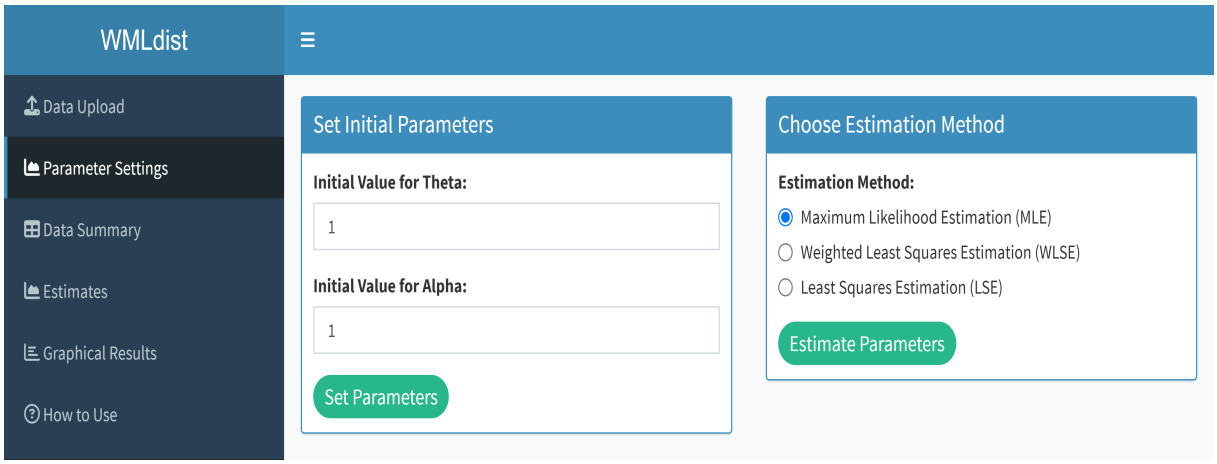

Figure 7. Parameter settings panel.

WMLdist allows the applicability of three different parameter estimation methods. These are the MLE, WLSE, and LSE methods. The Nelder-Mead algorithm is used for parameter estimation. This algorithm is sensitive to the initial values of the parameters. In WMLdist, the user has the possibility to change the initial values of the parameters (see Figure 7).

WMLdist also provides the descriptive statistics and some useful plots of the data used. The empirical hazard structure of the data is analyzed with the total test time (TTT) plot [24], outliers are analyzed with a violin plot, and skewness is analyzed with a histogram. In addition, descriptive statistics for the data are also shown in WMLdist (see Figure 8).

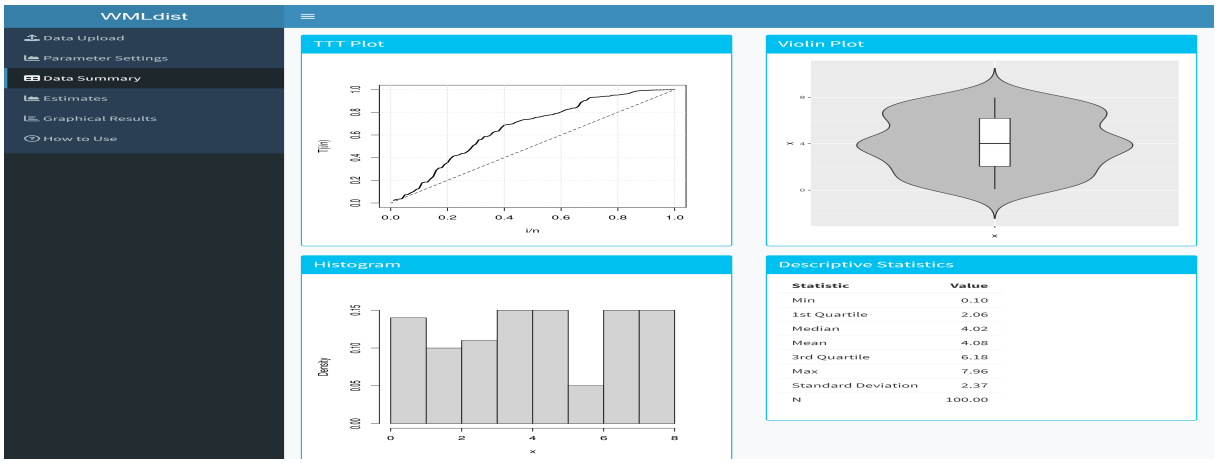

Figure 8. Data summary panel.

The values of the estimated parameters and goodness-of-fit test results obtained with the MLE, WLSE, and LSE methods are given in the Estimates section (see Figure 9).

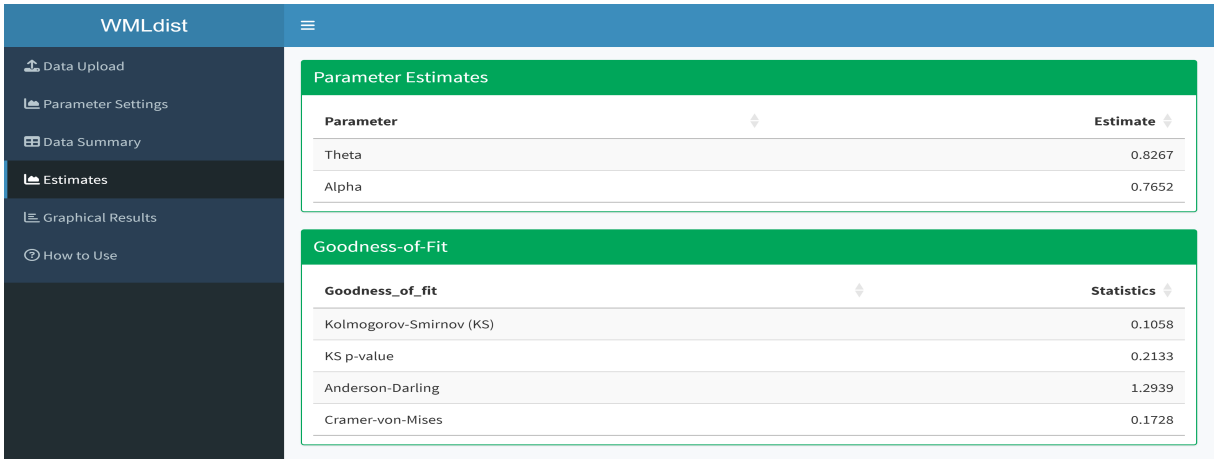

Figure 9. Estimates panel.

After obtaining the parameter estimates, a graphical examination of the fit of the WML distribution to the data is analyzed using density, hazard, and survival functions. The PP plot is also given (see Figure 10).

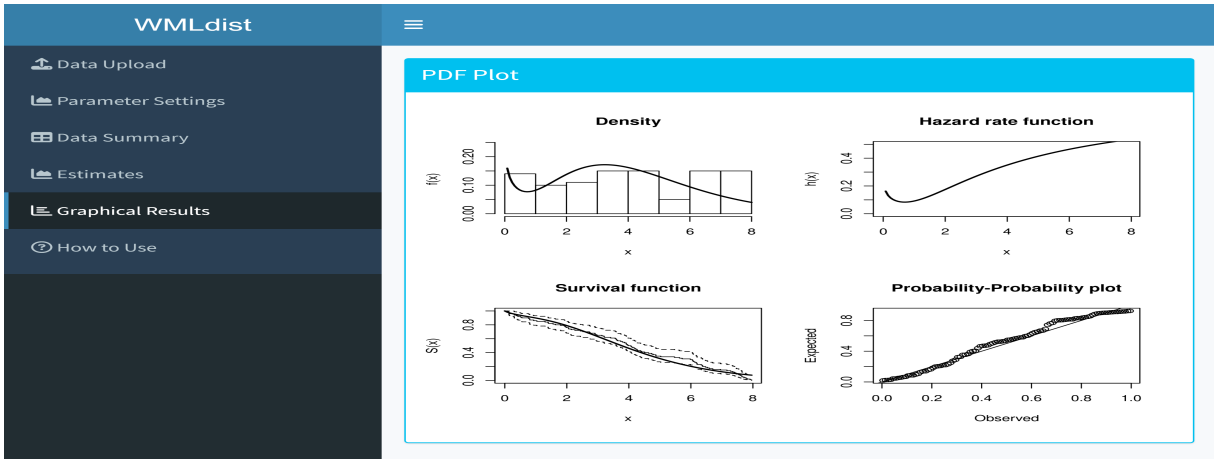

Figure 10. Graphical results panel.

Detailed information on the use of WMLdist is given in the help page (see Figure 11).

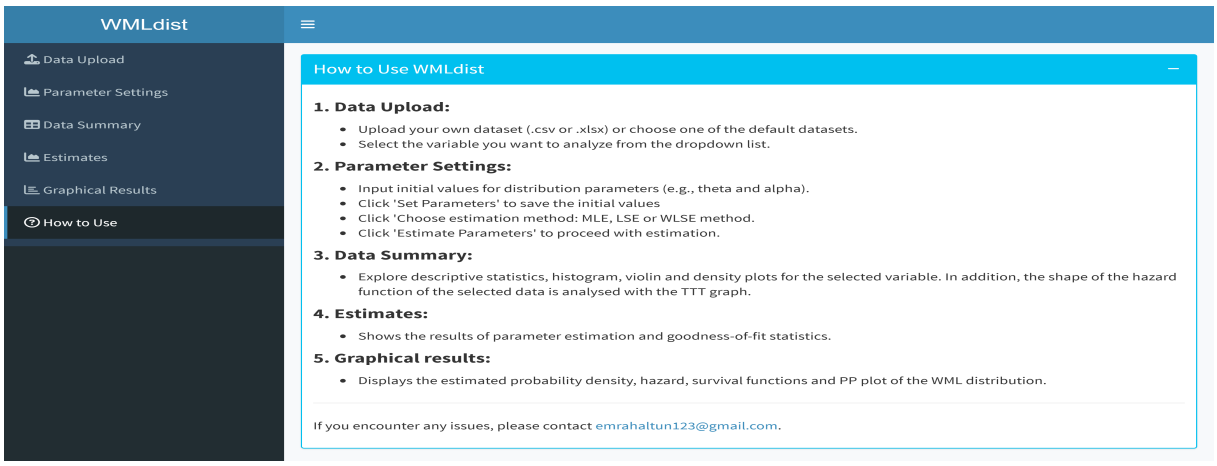

Figure 11. Help page panel.

6. Conclusions

In this study, a generalization of the MoL distribution is obtained with a weighted function, and the new distribution is called the WML distribution. The parameter estimates and statistical properties of the WML distribution are obtained, and the applications of the proposed distribution on real datasets reveal the applicability of the distribution in real life. Although many new distributions have been proposed, the applicability of these distributions is still limited. Thanks to the WMLdist web application provided in the study, the proposed model is available to all practitioners.

Use of AI tools declaration

The authors declare they have not used Artificial Intelligence (AI) tools in the creation of this article.

Acknowledgments

The researchers would like to thank the Deanship of Graduate Studies and Scientific Research at Qassim University for financial support (QU-APC-2025).

Conflict of interest

The authors declare there are no conflicts of interest.

References

1. E. Altun, G. Altun, The Maxwell-Boltzmann-Exponential distribution with regression model, *Math. Slovaca*, **74** (2024), 1011–1022. https://doi.org/10.1515/ms-2024-0074
2. E. Altun, M. C. Korkmaz, M. El-Morshedy, M. S. Eliwa, The extended gamma distribution with regression model and applications, *AIMS Math.*, **6** (2021), 2418–2439. https://doi.org/10.3934/math.2021147
3. R. D. Gupta, D. Kundu, Theory & methods: Generalized exponential distributions, *Aust. N. Z. J. Stat.*, **41** (1999), 173–188. https://doi.org/10.1111/1467-842X.00072
4. E. W. Stacy, A generalization of the gamma distribution, *Ann. Math. Stat.*, **33** (1962), 1187–1192.
5. W. Wang, Y. Li, N. Ikegaya, Statistical models incorporating mean and standard deviation to predict probability distributions of pedestrian-level wind speed in a realistic urban area, *Build. Environ.*, **279** (2025), 113034. https://doi.org/10.1016/j.buildenv.2025.113034
6. Y. Chen, M. Zhao, Z. Liu, J. Ma, L. Yang, Comparative analysis of offshore wind resources and optimal wind speed distribution models in China and Europe, *Energies*, **18** (2025), 1108. https://doi.org/10.3390/en18051108
7. P. Lencastre, A. Yazidi, P. G. Lind, Modeling wind-speed statistics beyond the Weibull distribution, *Energies*, **18** (2024), 2621. https://doi.org/10.3390/en17112621
8. O. Mykhailenko, N. Karabut, V. Doskoch, O. Burtseva, V. Kuznetsov, S. Tsvirkun, et al., Modeling of wind speed distribution in Urban environment for the application of wind energy potential estimation: Case study, *TEM J.*, **14** (2025), 107–116. https://doi.org/10.18421/TEM141-10
9. W. A. Marambakuyana, S. C. Shongwe, Quantifying risk of insurance claims data using various loss distributions, *J. Stat. Appl. Pro.*, **13** (2024), 1031–1044. http://doi.org/10.18576/jsap/130315
10. J. Hengcharoensuk, A. Moumeesri, Ruin probability analysis in automobile insurance using gamma-Cubic transmuted exponential distribution for claim severity, *Int. J. Math. Eng. Manage. Sci.*, **10** (2025), 486–505. https://doi.org/10.33889/IJMEMS.2025.10.2.024
11. H. M. Yousof, E. I. Ali, K. Aidi, N. S. Butt, M. M. Saber, A. H. Al-Nefaie, et al., The statistical distributional validation under a novel generalized gamma distribution with value-at-risk analysis for the historical claims, censored and uncensored real-life applications, *Pak. J. Stat. Oper. Res.*, **21** (2025), 51–69.

12. M. Salajegheh, M. J. Nooghabi, K. Okhli, A Bayesian approach for modeling heavy tailed insurance claim data based on the contaminated lognormal distribution, *METRON*, **83** (2025), 213–234. https://doi.org/10.1007/s40300-025-00288-9
13. A. Putri, Estimation model of pure health insurance premiums in Southeast America using generalized linear model (GLM) with gamma distribution, *Int. J. Bus. Econ. Social Dev.*, **6** (2025), 44–51. https://doi.org/10.46336/ijbesd.v6i1.873
14. A. S. Rizal, D. D. Prastyo, Bivariate poisson inverse gamma INAR (1) regression model: Healthcare service visits by health insurance members case study, in *9th International Conference on Business and Industrial Research*, IEEE, (2024), 1384–1389. https://doi.org/10.1109/ICBIR61386.2024.10875799
15. Y. Zhou, Y. J. Zhang, Physical controls and regional pattern similarities of precipitation and flow duration curves using the three-parameter gamma distribution, *Hydrol. Processes*, **38** (2024), e15082. https://doi.org/10.1002/hyp.15082
16. R. Montes-Pajuelo, A. M. Rodriguez-Perez, R. Lopez, C. A. Rodriguez, Analysis of probability distributions for modelling extreme rainfall events and detecting climate change: Insights from mathematical and statistical methods, *Mathematics*, **12** (2024), 1093. https://doi.org/10.3390/math12071093
17. A. I. Shah, N. D. Pan, Evaluation of probability distribution methods for flood frequency analysis in the Jhelum Basin of North-Western Himalayas, India, *Cleaner Water*, **2** (2024), 100044. https://doi.org/10.1016/j.clwat.2024.100044
18. N. F. E. M. Johar, A. Senawi, N. A. A. A. Ghani, An assessment of rainfall distribution in Kuantan river basin using generalized extreme value distribution and Gamma distribution, *AIP Conf. Proc.*, **2895** (2024), 090033. https://doi.org/10.1063/5.0192286
19. S. Karuppusamy, V. Balakrishnan, K. Sadasivan, Modified one-parameter Lindley distribution and its applications, *Int. J. Eng. Res. Appl.*, **8** (2018), 50–56.
20. M. E. Ghitany, F. Alqallaf, D. K. Al-Mutairi, H. A. Husain, A two-parameter weighted Lindley distribution and its applications to survival data, *Math. Comput. Simul.*, **81** (2011), 1190–1201. https://doi.org/10.1016/j.matcom.2010.11.005
21. E. Altun, C. Chesneau, H. N. Alqifari, Two parameter log-Lindley distribution with LTPL web-tool, *AIMS Math.*, **10** (2025), 8306–8321. https://doi.org/10.3934/math.2025382
22. G. Altun, E. Altun, S. Islamoglu, Displaying bivariate data with developed cloud based data visualization tool, *Konuralp J. Math.*, **12** (2024), 150–157.
23. E. Altun, M. El-Morshedy, SimBetaReg web-tool: The easiest way to implement the beta and simplex regression models, *Symmetry*, **13** (2021), 2437. https://doi.org/10.3390/sym13122437
24. M. V. Aarset, How to identify a bathtub hazard rate, *IEEE Trans. Reliab.*, **R-36** (1987), 106–108. https://doi.org/10.1109/TR.1987.5222310

AIMS Press